Article

Robust Motion Planning in Robot-Assisted Surgery for Nonlinear Incision Trajectory

Shailu Sachan *[ID] and Pankaj Swarnkar

Department of Electrical Engineering, Maulana Azad National Institute of Technology, Bhopal 462003, India
* Correspondence: sachanshailu@gmail.com

Abstract: In the era of digital OTs (operating theatres), the developments in robot-assisted surgery (RAS) can greatly benefit the medical field. RAS is a method of technological advancement that uses robotic articulations to assist in complicated surgeries. Its implementation improves the ability of the specialized doctor to perform surgery to a great extent. The paper addresses the dynamics and control of the highly non-linear 3DOF surgical robot manipulator in the event of external disturbances and uncertainties. The integration of non-linear robust SMC (sliding mode control) with a smoothing mechanism, a FOPID (fractional-order proportional integral derivative) controller, and a fuzzy controller provides a high degree of robustness and minimal chatter. The addition of fuzzy logic to the controller, named intelligent fuzzy-SFOSMC (smoothing fractional order sliding mode controller) improves the system's performance by ruling out the disturbances and uncertainties. The prototype model is developed in a laboratory and its outcomes are validated on OP5600, a real-time digital simulator. Simulation and experimental results of the proposed fuzzy-SFOSMC are compared with conventional controllers, which illustrates the efficacy and superiority of the proposed controller's performance during the typical surgical situations. The proposed fuzzy-SFOSMC outperforms conventional controllers by providing greater precision and robustness to time-varying nonlinear multi-incision trajectories.

Keywords: fractional-order proportional integral derivative (FOPID); real-time digital simulator; robot-assisted surgery (RAS); sliding mode control (SMC); surgical robot manipulator; fuzzy

1. Introduction

Medical robotics is closely linked to human health. Day by day, the use of robotics in medicine is becoming widespread as it has different benefits in the medical profession. In recent years, RAS has proven to be a booming field. The introduction of robotics into the medical field has substituted the traditional surgical course of action. To carry out difficult, minimally invasive surgical (MIS) operations, surgical robots [1] have high precision and dexterity. The efficacy and scope of MIS is improved by surgical robotics as some of the advantages of robotic surgery include the requirement for smaller incisions, greater precision and capacity to replicate identical movements, reduced bleeding, reduced pain, reduced scarring, quicker healing period and a shorter stay in the hospital [2]. In the 1960s, NASA introduced telerobotics for surgery for different uses, such as assistive devices and supporting manipulators, for the first time. Their objective was to provide astronauts with medical assistance [3].

Owing to coupling and nonlinearity effects in the robotic system, apt motion control for surgical robots is a difficult task [4]. For surgical robots, a novel control is presented in this paper. SMC is an efficient robust nonlinear control because of its invariance properties towards the system. It deals with the design of the controller to handle uncertainties to achieve robust performance and stability under various assumptions to track the system's time varying trajectory [4–6].

SMC offers robustness and satisfactory monitoring efficiency of disturbances [7,8]. However, it has many drawbacks, e.g., the optimum sliding surface selection is intricate, it is sensitive to noise, chattering causes saturation and heating in the different mechanical parts of a surgical robot, and it has composite non-linear dynamics [6,9,10]. Even if the PID controllers have low tracking performance, they offer better reliability and stability than the SMC controller. Thus, the combination of the advantages of both PID and SMC control guarantees stability and good monitoring performance. As a result of an increased number of gain parameters, FOPID controllers [11,12] are superior to PID controllers, as they improve efficiency and flexibility. The coupling of FOPID and SMC would consequently be helpful in increasing the efficiency and robustness of the system [6,13].

Conventional controllers work well for single incisions and linear trajectories. In the case of time-varying and nonlinear trajectories, conventional controllers fail. Chattering, however, remains the major hindrance to the application of sliding mode control and prominently impairs the controlled manipulator's tracking performance. The chatter obtained through SMC is attenuated by the smoothing function and the fuzzy logic controller [14–17]. Fuzzy logic controllers (FLC) are intelligent controllers that quantify linguistic variables using fuzzy logic. It imitates the human decision-making process. They are used in energy management, smart watering system, robots, autonomous vehicles, etc. [18–20]. FLCs combined with SMC have also been found to be efficient in other applications such as vehicles [21–23], robots [4,24], communication [25], converters [26], etc. The amalgamation of fuzzy logic and smoothing fractional order SMC enhances performance, increases precision, and eliminates chattering for nonlinear multi-incision trajectories when compared to the conventional sliding mode control methodologies. Therefore, this paper proposes fuzzy-SFOSMC for 3DOF master-slave surgical robots for the application of RAS. Detailed simulation work has been carried out in the MATLAB Simulink environment for this practical purpose. Additionally, the gain parameters of controllers were found using PSO [27–30] (particle swarm optimization). PSO offers a number of benefits over other optimization methods, including ease of implementation, fewer parameters, faster convergence, and efficiency [28]. Additionally, the prototype model has been developed in a laboratory and the results of trajectory tracking with chatter reduction have been validated in real time using OP5600 (Opal-RT: a real-time digital simulator).

The major contributions of the paper are as follows:

(1) Surgical robot dynamics with robust controllers;
(2) Design, implementation, and validation of controllers for robust tracking during typical surgical situations using OP5600;
(3) The proposed fuzzy-SFOSMC is compared with the existing traditional SMCs based on the time response parameters for time-varying nonlinear multi-incision trajectories in the presence of uncertainties.

The paper is structured in the following way: Section 2 discusses the 3DOF surgical robot manipulator model. In Section 3, the different controllers for surgical manipulator are conferred, Section 4 illustrates and discusses simulation results, then, experimental validation is performed on OP5600, i.e., a real-time digital simulator, in Section 5. Additionally, the last section concludes the paper's work.

2. Surgical Robot's Dynamic Model

The paper emphasizes on motion control of surgical robots, as illustrated in Figure 1. This motion-controlled manipulator will be of great help in surgical processes. Each joint of the surgical manipulator provides relative motion between the links. The different controllers are intended to control the position of the surgical manipulator.

CSMC offers robustness and satisfactory monitoring efficiency tofo disturbances [7,8]. However, it has many drawbacks, including intricate optimum sliding surface selection, sensitivity to noise, chattering which causes saturation and heating in the different mechanical parts of a surgical robot, and composite non-linear dynamics [6,9,10]. Even if PID controllers have a low tracking performance, they offer better reliability and stability

than the SMC controller. Thus, the combination of the advantages of both PID and SMC controllers, known as PID-SMC, guarantees stability and good monitoring performance. As a result of the increased number of gain parameters, FOPID controllers [11,12] are superior to PID controllers, improving efficiency and flexibility. The coupling of FOPID and SMC, known as FOPID-SMC, would consequently be helpful in increasing the efficiency and robustness of the system [6,13].
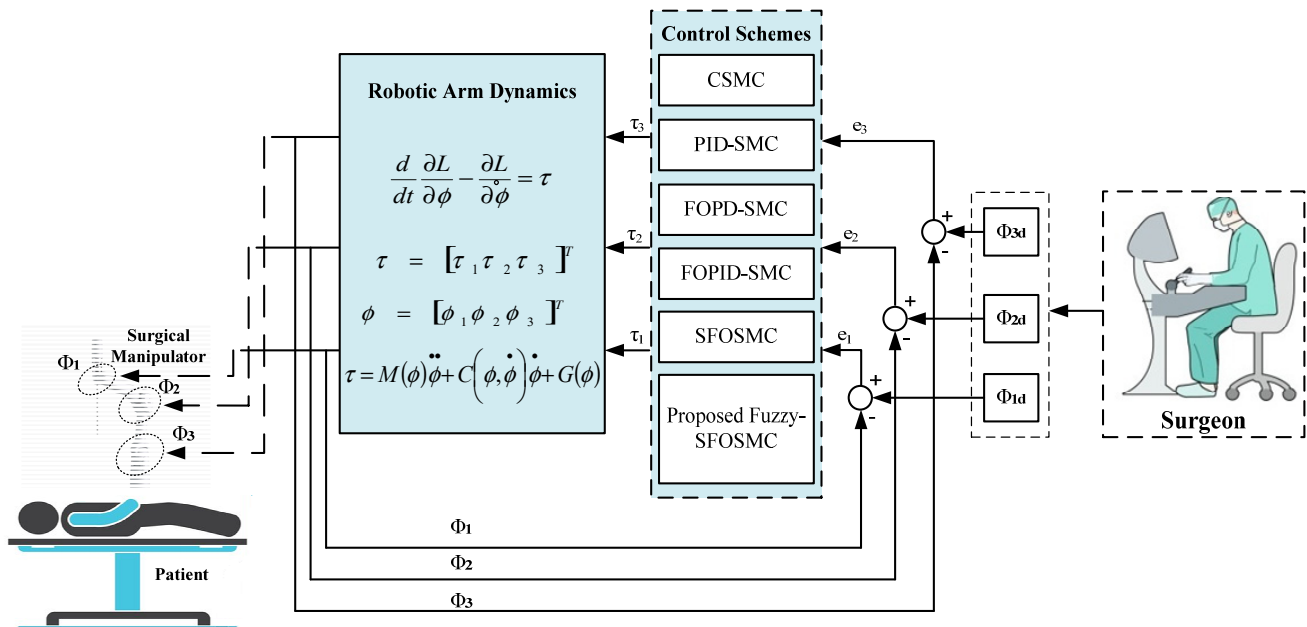

Figure 1. Outline of this work.

Conventional controllers work well for single incisions and linear trajectories. In the case of time-varying and nonlinear trajectories, conventional controllers fail. Chattering, however, remains the major hindrance to the application of sliding mode control and prominently impairs the controlled manipulator's tracking performance. The chatter obtained through CSMC is attenuated by the smoothing function and the fuzzy logic controller [14–17]. SFOSMC is the combination of FOPID-SMC and smoothing function. Fuzzy logic controllers (FLC) are an intelligent controller that quantify linguistic variables using fuzzy logic. They imitate the human decision-making process. FLCs combined with SMC have also been found to be efficient in other applications such as vehicles [21–23], robots [4,24], communication [25], converters [26], etc. The amalgamation of fuzzy logic and smoothing fractional order SMC enhances performance, increases precision, and eliminates chattering for nonlinear multi-incision trajectories compared to the conventional sliding mode control methodologies. PSO optimizes the controller parameters in conjunction with advanced and robust AI control techniques. As a result, this paper proposes a combined PSO optimized fuzzy-SFOSMC for 3DOF master-slave surgical robots for RAS applications to achieve errorless operation, which is essential. The various controllers used to control the position of the surgical manipulator are discussed in detail in the following section.

The dynamic model of a three links-three joints surgical robot manipulator is represented in Figure 2. The basics of the dynamics of the manipulator are well known and are more specifically represented by the below derivation. For an n-DOF robot manipulator, the Euler–Lagrange equation is [4]:

$$\tau = M(\phi)\ddot{\phi} + C\left(\phi, \dot{\phi}\right)\dot{\phi} + G(\phi) + \tau_d\left(\phi, \dot{\phi}\right) \tag{1}$$

where $\phi, \dot{\phi}, \ddot{\phi}$ denote the position, velocity, and acceleration of manipulator's joint. τ is the input control torque, $M(\phi)$ is the inertia matrix, $G(\phi)$ is the gravity vector, $C\left(\phi, \dot{\phi}\right)$ is the coriolis/centripetal n and $\tau_d\left(\phi, \dot{\phi}\right)$ is the disturbance vector.

$$\ddot{\phi} = -M^{-1}(\phi)C\left(\phi, \dot{\phi}\right)\dot{\phi} - M^{-1}(\phi)G(\phi) - d(t) + M^{-1}(\phi)\tau$$
$$\ddot{\phi} = -(A + \Delta A)\dot{\phi} - (B + \Delta B)G(\phi) - d(t) + (D + \Delta D)w(t) \tag{2}$$

where ΔA, ΔB, and ΔD are the uncertainties present in the system, $A = M^{-1}(\phi)C\left(\phi, \dot{\phi}\right)$,

$B = D = M^{-1}(\phi)$, $d(t) = M^{-1}(\phi)\left(\tau_d\left(\phi, \dot{\phi}\right)\right)$, and $w(t) = \tau$. For a 3DOF surgical manipulator,

$$\phi = [\phi_1 \phi_2 \phi_3]^T \tau = [\tau_1 \tau_2 \tau_3]^T$$

where ϕ_3 is the angle between the base and first link of the robotic manipulator, ϕ_2 is the angle between second link and first link of the robotic manipulator, and ϕ_1 is the angle between third link and second link of the robotic manipulator. τ_1, τ_2, and τ_3 are the resultant torques applied to joint1, joint2, and joint3, respectively, of the surgical manipulator.
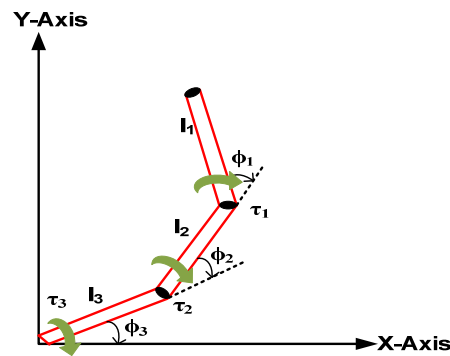

Figure 2. 3DOF robotic manipulator.

3. Different Controllers for Surgical Manipulator

Various controllers are designed to control the joints' position, which causes torque to be generated and applied to the surgical manipulator's joints as presented in Figure 1. These are discussed in detail below.

3.1. CSMC (Conventional Sliding Mode Controller)

CSMC [6,10] is a non-linear controller applicable to nonlinear MIMO (Multiple-Input-Multiple-Output) systems. It deals with uncertain systems and withstands external disturbances [8,9]. Since CSMC offers robustness and stability, its inclusion in a surgical robot is required. Robotic control with CSMC is a good approach to solve set-point problems [5].

It is well known that two important phases in the development of a sliding mode controller are the selection of a sliding surface (σ) and the development of the control law (u). The purpose of the CSMC is to push the tracking error (e) towards the 'σ' and then transfer the error to the origin along the sliding surface. Therefore, the tracking error is specified by:

$$e = \phi_d - \phi,$$

where ϕ is the actual trajectory and ϕ_d is the desired trajectory. The CSMC has a PD-based sliding surface that has proportional (K_p) and derivative (K_d) terms to respond rapidly to an error change, which are specified by [6,10]:

$$\sigma = K_p e + K_d \dot{e}.$$

As is well-known, the control law of CSMC is the combination of reaching control ($u_r(t)$) and equivalent control ($u_{eq}(t)$) and is given as [5]:

$$u(t) = u_{eq}(t) + u_r(t). \tag{3}$$

To determine the equivalent control, take the derivative of sliding surface, i.e.,

$$\dot{\sigma} = K_p \dot{e} + K_d \ddot{e}.$$

The equivalent torque is given by:

$$u_{eq} = g^{-1}(\phi)\left[-f(\phi) + \ddot{\phi}_d + \lambda\sigma\right], \tag{4}$$

where $f(\phi) = -M^{-1}(\phi)\left[C(\phi,\dot{\phi}) + G(\phi)\right]$ and $g(\phi) = M^{-1}(\phi)$.

Additionally, the reaching control of the control law is given by:

$$u_r = K sign(\sigma). \tag{5}$$

Now, the computed torque control law [6] from Equations (3)–(5) is:

$$\tau = g^{-1}(\phi)\left[-f(\phi) + \ddot{\phi}_d + \lambda\sigma + K sign(\sigma)\right] \tag{6}$$

The four traditional controllers, i.e., CSMC, PID-SMC, FOPD-SMC, and FOPID-SMC are shown in Figure 3 and discussed in our previous paper [6].
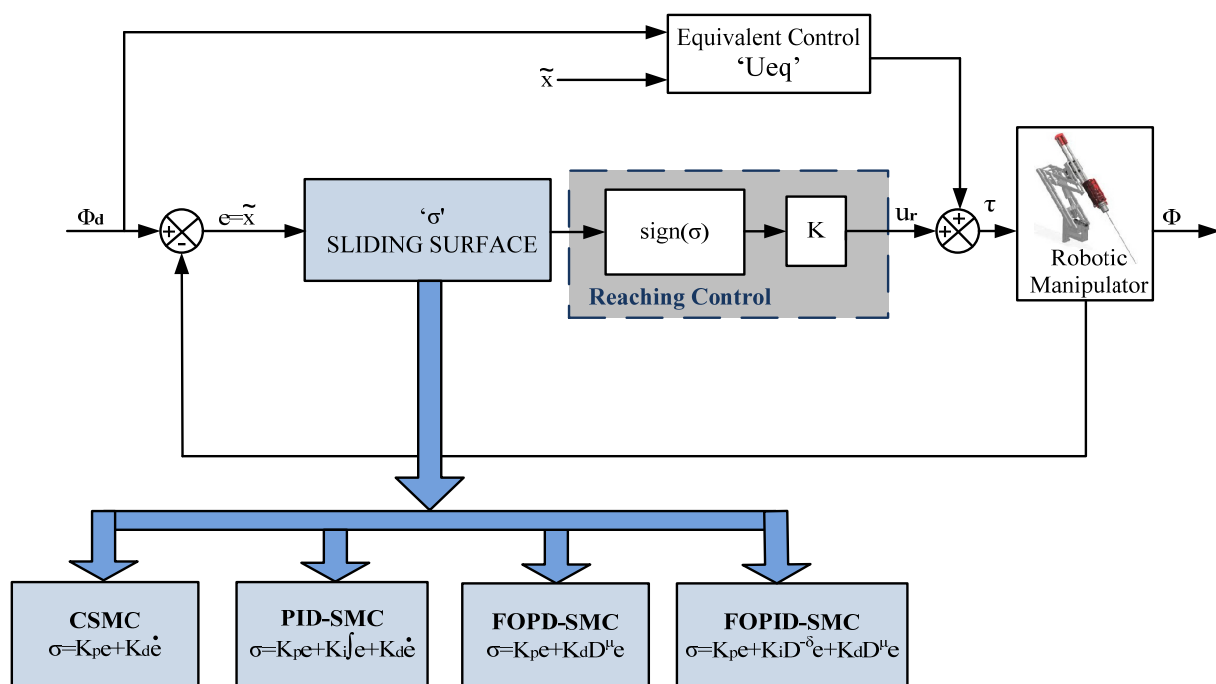

Figure 3. Conventional SMC controllers for surgical manipulators.

3.2. PID-SMC

The PID-SMC [4,6] controller has a PID (Proportional Integral Derivative)-based sliding surface. The incorporation of the integral term into the sliding surface with the derivative term minimizes the error, specified by the following equation [6,12]:

$$\sigma = K_p e(t) + K_I \int e(t) + K_d \dot{e}(t). \tag{7}$$

Now, the computed torque control law for a 3DOF surgical robot from Equations (6) and (7) is:

$$\tau = g^{-1}(\phi)\left[-f(\phi) + \ddot{\phi}_d + \lambda\left(K_p e + K_I \int e + K_d \dot{e}\right) + K sign(\sigma)\right].$$

3.3. FOPD-SMC

The FOPD-SMC [6] controller has a FOPD (Fractional Order Proportional Derivative)-based sliding surface that has an additional fractional-order derivative. Its sliding surface is defined by [6]:

$$\sigma = K_p e + K_d D^\mu e.$$

Substitute the sliding surface 'σ' in Equation (6) to obtain the computed torque control law for 3DOF surgical manipulator:

$$\tau = g^{-1}(\phi)\left[-f(\phi) + \ddot{\phi}_d + \lambda\left(K_p e + K_d D^\mu e\right) + K sign(\sigma)\right].$$

3.4. FOPID-SMC

The FOPID-SMC controller has a sliding surface based on the FOPID (Fractional Order Proportional Integral Derivative) with proportional, derivative, and integral terms and two additional parameters viz. fractional integration order (δ) and fractional derivative order (μ) [6,11–13]. This integration of additional parameters enhances the system's accuracy and flexibility. The FOPID-based sliding surface is specified by [6,12]:

$$\sigma = K_p e + K_i D^{-\delta} e + K_d D^\mu e. \tag{8}$$

Substitute the sliding surface 'σ' in Equation (6) to get the computed torque control law for 3DOF surgical manipulator:

$$\tau = g^{-1}(\phi)\left[-f(\phi) + \ddot{\phi}_d + \lambda\left(K_p e + K_i D^{-\delta} e + K_d D^\mu e\right) + K sign(\sigma)\right].$$

3.5. SFOSMC (Smoothing Fractional Order SMC)

The conventional SMC has a discontinuous sign (σ) function that introduces oscillations into the system, which is an unwanted phenomenon called chattering. This causes the heating and saturation of the different mechanical parts of the surgical manipulator. The smoothing function, i.e., the saturation function (sat (σ)) is used to overcome this problem instead of the signum function, as it removes the chatter by integrating the boundary layer into the control [5,6,9].

This boundary layer introduction and chatter minimization in the FOPID-SMC is known as smoothing FOPID-SMC. In this paper, η (boundary layer thickness) is taken as 0.15 to mitigate the chattering. Therefore, the sat function [5,6] can be characterized as:

$$\text{sat}(\sigma) = \text{sign}(\sigma) \text{ for } |\sigma| > \eta \text{ and } sat(\sigma) = \frac{sign(\sigma)}{\eta} \text{ for } |\sigma| \leq \eta.$$

The computed torque controller for surgical manipulator is then given by:

$$\tau = g^{-1}(\phi)\left[-f(\phi) + \ddot{\phi}_d + \lambda\sigma + Ksat(\sigma)\right]. \tag{9}$$

From Equations (8) and (9):

$$\tau = g^{-1}(\phi)\left[-f(\phi) + \ddot{\phi}_d + \lambda\left(K_pe + K_iD^{-\delta}e + K_dD^\mu e\right) + Ksat(\sigma)\right].$$

The infinite switching introduces undesired chattering into the system. This chatter problem is alleviated by the implementation of fuzzy logic control. Therefore, the proposed fuzzy-SFOSMC controller was designed to make the system more robust and chatter free. The SFOSMC and proposed fuzzy-SFOSMC control schemes are shown in Figure 4.
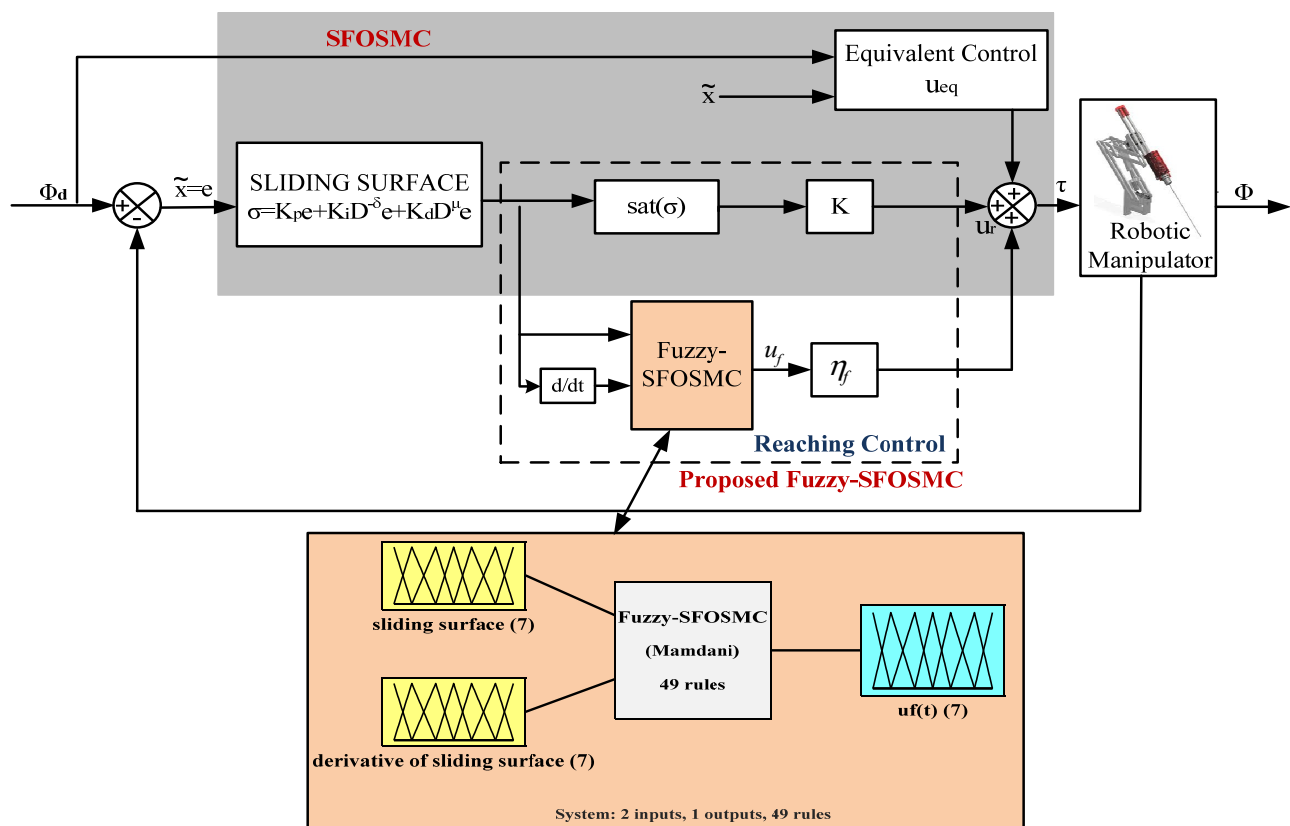
Figure 4. SFOSMC and proposed fuzzy-SFOSMC controllers for surgical manipulators.

3.6. Proposed Fuzzy-SFOSMC

The theory of Artificial Intelligence (AI) has been applied often in sliding mode-controlled systems in recent years. One of the more prominent implementations of fuzzy logic theory is the FLC (fuzzy logic controller) [14–17]. Fuzzy logic controllers (FLC) are intelligent controllers that quantify linguistic variables using fuzzy logic. It imitates the human decision-making process. They are used in energy management, smart watering systems, robots, autonomous vehicles, etc. [18–20]. Uncertain, noisy, and non-linear systems can be brought under control with this controller. FLCs combined with SMC have also been found to be efficient in other applications such as vehicles [21–23], robots [4,24], communication [25], converters [26], etc. The blending of FLC and SFOSMC is referred as proposed fuzzy-SFOSMC (Figure 4) which includes the advantages and features of both the controllers. The amalgamation of fuzzy logic and smoothing fractional order SMC enhances

performance, increases precision, and eliminates chattering for nonlinear multi-incision trajectories compared to the conventional sliding mode control methodologies.

The FLC consists of a fuzzifier (binary to fuzzy conversion), fuzzy rules, an inference engine, and a defuzzifier (fuzzy to binary conversion). The Mamdani fuzzy inference engine is used in this paper to alleviate chattering. The max-min aggregation and the centroid method are used for defuzzification. The reaching control law of a fuzzy controller is specified by:

$$u'_r(t) = \eta_f u_f(t)$$

where $u_f(t)$ is the output of fuzzy-SFOSMC and $\eta_f(t)$ is the normalizing factor. $u_f(t)$ is the normalization of a sliding surface and the derivative of a sliding surface. The input and output MFs (membership functions) of the fuzzy-SFOSMC are 2D functions as presented in Figure 5a–c, respectively. The input and output MFs are further split into seven fuzzy sets that are "PS (Positive small), PM (Positive medium), PB (Positive big), Z (Zero), NM (Negative medium), NB (Negative big), and NS (Negative small)" [4].
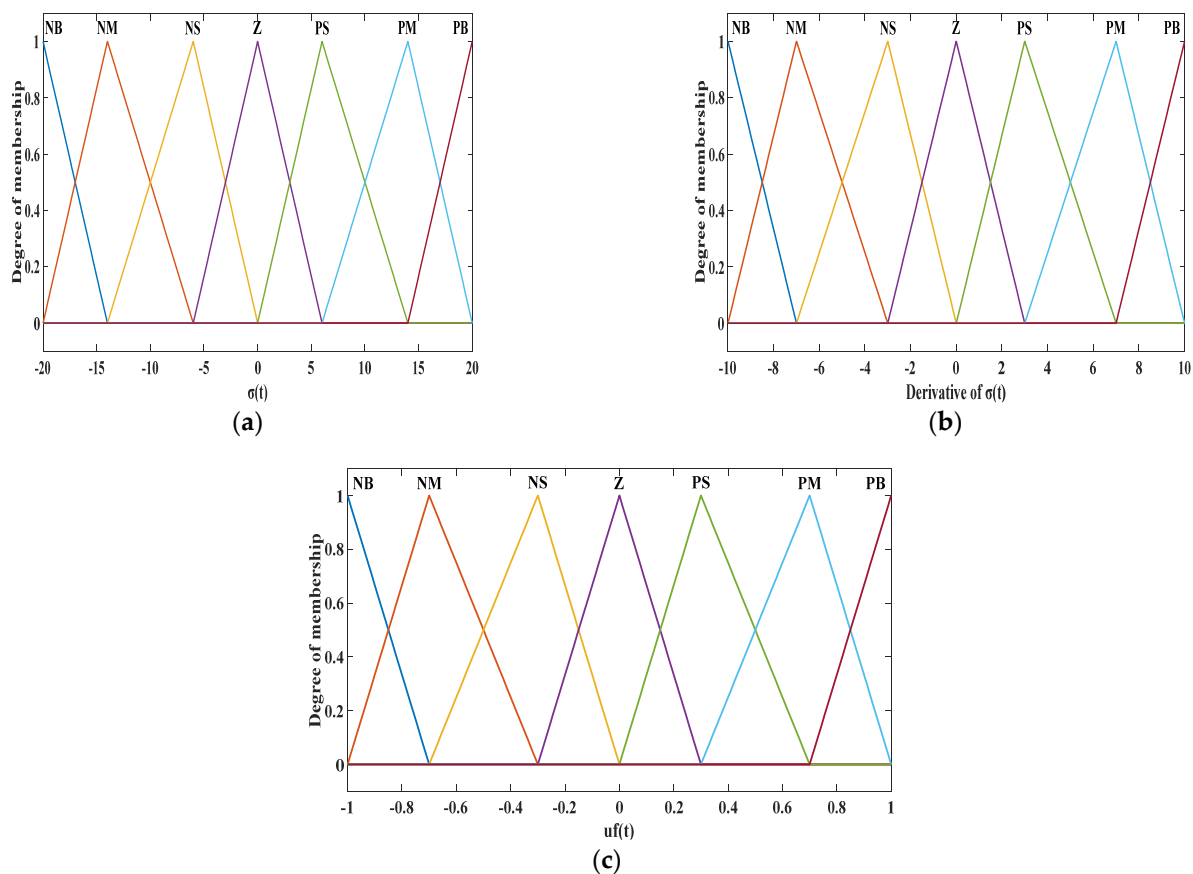
Figure 5. Fuzzy−SFOSMC Parameters. (**a**) Input1 MF. (**b**) Input2 MF. (**c**) Output MF.

These fuzzy membership functions are defined in the fuzzy rules:

$R^{(i)}$:: IF $\sigma(t)$ is A_1^i and $\overset{\bullet}{\sigma}(t)$ is A_2^i THEN $u_f(t)$ is $B^{(i)}$

where A_1^i and A_2^i are the input fuzzy set labels and B^i is the output fuzzy set label. The rule matrix table for the fuzzy-SFOSMC's reaching control is displayed in Table 1.

Table 1. Rule matrix for the proposed fuzzy-SFOSMC.

$\sigma(t)$ / $\sigma(t)$	NB	NM	NS	Z	PS	PM	PB
NB	NB	NB	NB	NB	NM	NS	Z
NM	NB	NB	NB	NM	NS	Z	PS
NS	NB	NB	NM	NS	Z	PS	PM
Z	NB	NM	NS	Z	PS	PM	PB
PS	NM	NS	Z	PS	PM	PB	PB
PM	NS	Z	PS	PM	PB	PB	PB
PB	Z	PS	PM	PB	PB	PB	PB

The complete fuzzy-SFOSMC control law is computed as:

$$u(t) = u_{eq}(t) + u_r(t) = u_{eq}(t) + \eta_f \cdot u_f(t) + Ksat(\sigma) \tag{10}$$

where $u_r(t) = u'_r(t) + Ksat(\sigma)$ and σ is the FOPID-based sliding surface, whose parameters (K_P, K_I, K_D, μ, and δ) are found using PSO [27–30]. PSO offers a number of benefits over other optimization methods, including ease of implementation, fewer parameters, faster convergence, and higher efficiency. The objective of PSO is to minimize the error; therefore, its objective function is represented by:

$$O = \int e^2 \tag{11}$$

4. Materials and Methods

All of the six controllers discussed were implemented during surgery for a typical situation. It can be clearly seen that the results of the SMC controllers have a chattering problem. This is resolved by using the proposed fuzzy-SFOSMC controller, as chattering is eliminated due to the existence of a saturation function and FLC.

Conventional controllers work well for single incisions and linear trajectories. In the case of time-varying and nonlinear trajectories, conventional controllers fail. Even chattering in the transient period degrades the performance of conventional controllers. Multiple incisions must be performed on the patient where incision time and depth of incision must be considered. For simulating these surgical situations with nonlinear incision trajectories, an intelligent fuzzy-SFOSMC is implemented in a master-slave surgical robot. In order to check the transient response of the slave, quick transmission from one incision to another is applied on the patient. Fast response time, precise incision at appropriate location, and chatter-free operation are the essential requirements for the case under study. That is why an intelligent nonlinear fuzzy-SFOSMC control methodology has been developed, implemented, and validated on the prototype model for ensuring a satisfactory performance of the master-slave surgical robot.

The predefined trajectories provided by the master robot to the 3DOF-slave robot during surgery are as follows: Φ1d = 1 + tanh(5*cos(2.5*(u − 0.5))), Φ2d = 1 + tanh(5*cos(2.5* (u − 1))), and Φ3d = 1 + tanh(5*cos(2.5*(u − 1.5))) [5]. The slave robot will follow these nonlinear trajectories efficiently.

For Validation on OP5600 (Real-Time Digital Simulator)

The OP5600 is a real-time, high-performance digital simulator. It has a multicore processor and digital and analog I/O channels. It is equipped with a fast Xilinx Artix-7 FPGA that provides supremacy in simulations and enhances the accuracy of the system. The multiple-core processor allows the simulation to execute at very high speeds.

The host system was installed with Opal-RT software, i.e., RT-LAB. RT-LAB was integrated with MATLAB Simulink and the system was connected to an OP5600 digital simulator via the ethernet. A DSO (Digital Storage Oscilloscope) DL750 was connected to the OP5600 via probes which captured the results as illustrated in Figure 6.
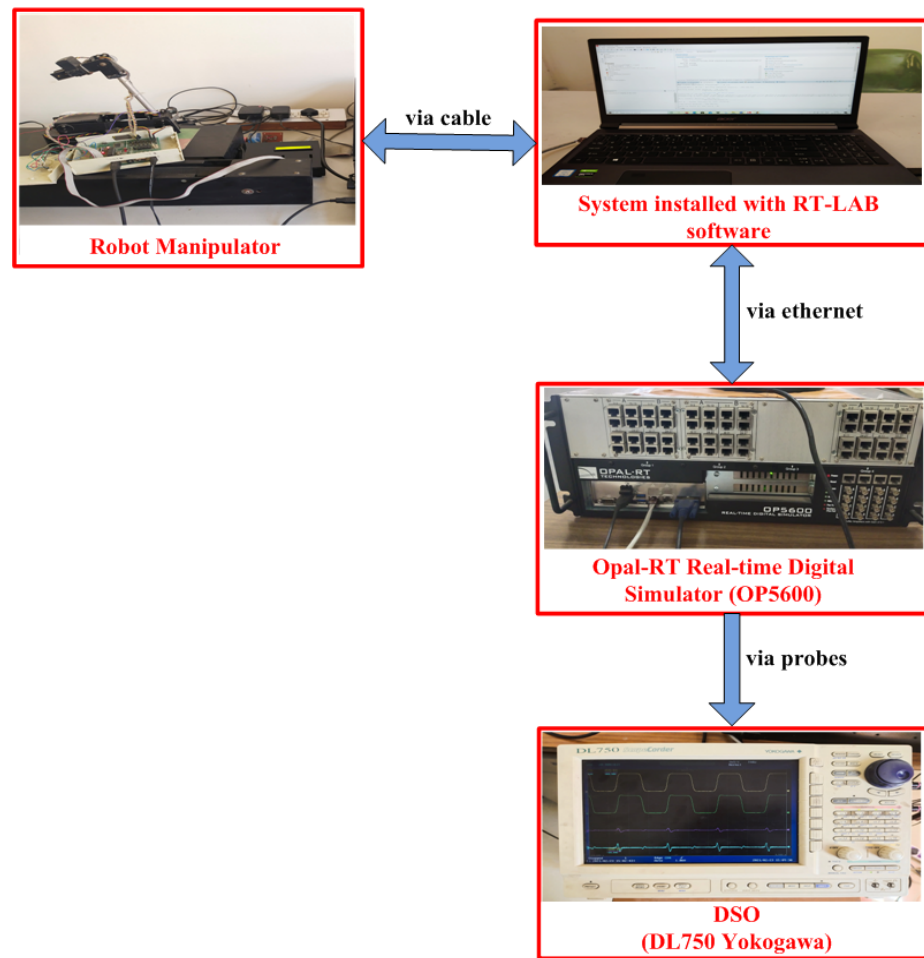
Figure 6. Experimental setup.

5. Results and Discussion

The slave robot follows the master robot's commands successfully. O is the initial position of the slave robot. It takes 0.25 s to move the tool to the body, 1 s to make the incision, 0.25 s to retract the tool, and 1 s to move the tool from O to P in Figure 7.
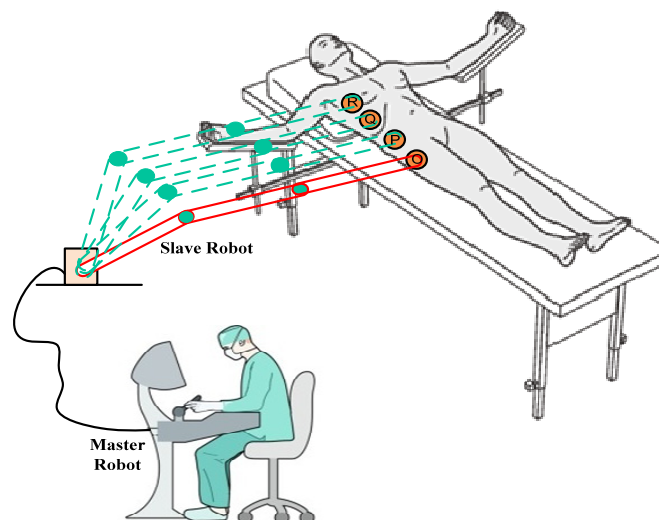

Figure 7. Case study for RAS with nonlinear incision trajectory.

5.1. Typical Situation during Surgery

The simulation results of the 3DOF surgical manipulator are shown in Figures 8–10, representing trajectory tracking, tracking errors, and sliding surfaces of the manipulator, respectively. It is observed that the proposed fuzzy-SFOSMC has better tracking compared to other controllers (CSMC, PID-SMC, FOPD-SMC, FOPID-SMC, and SFOSMC) as it has minimum overshoot and minimum tracking error.
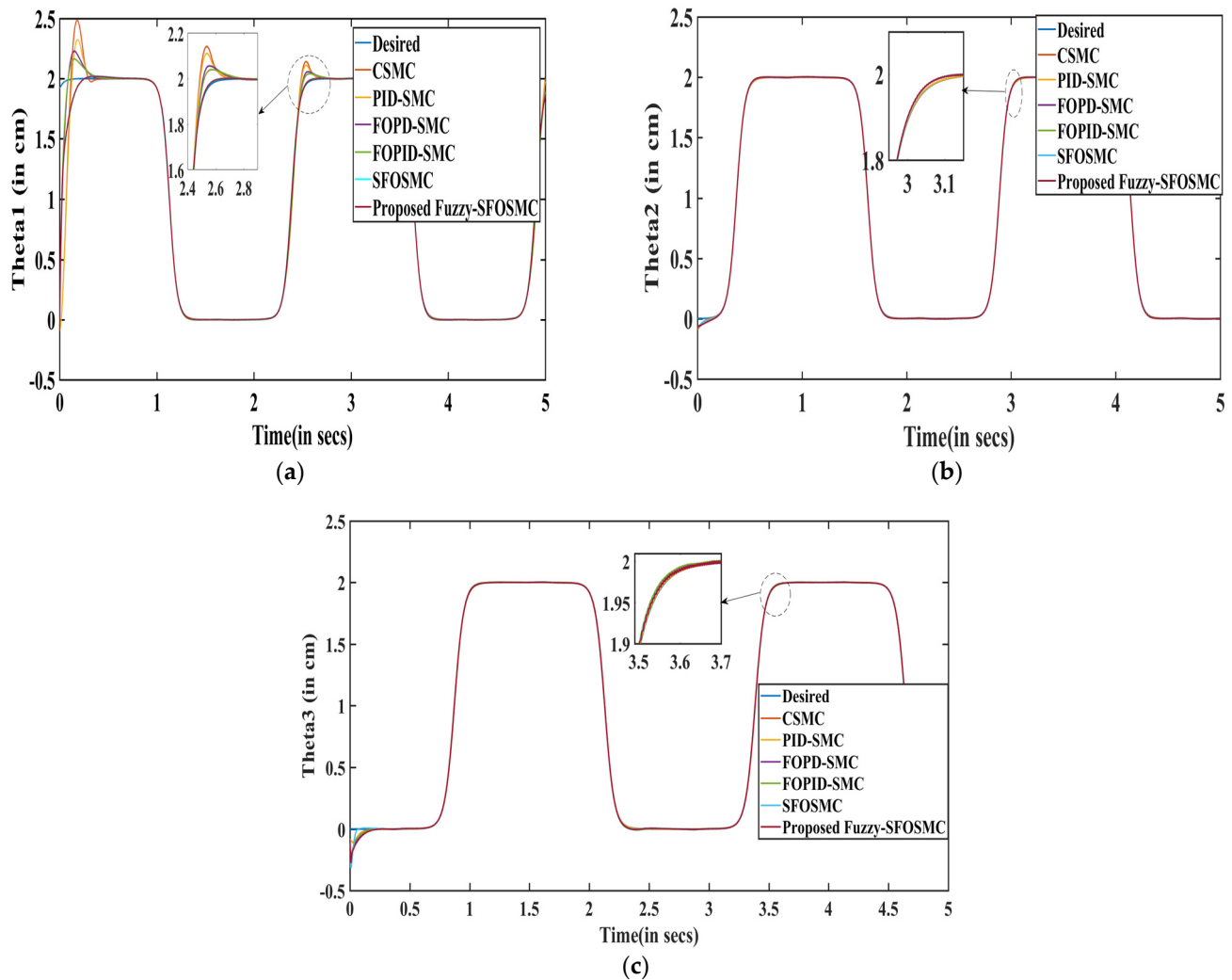
Figure 8. Trajectory tracking of the 3DOF surgical manipulator for Joint1 (**a**), Joint2 (**b**), and Joint3 (**c**).
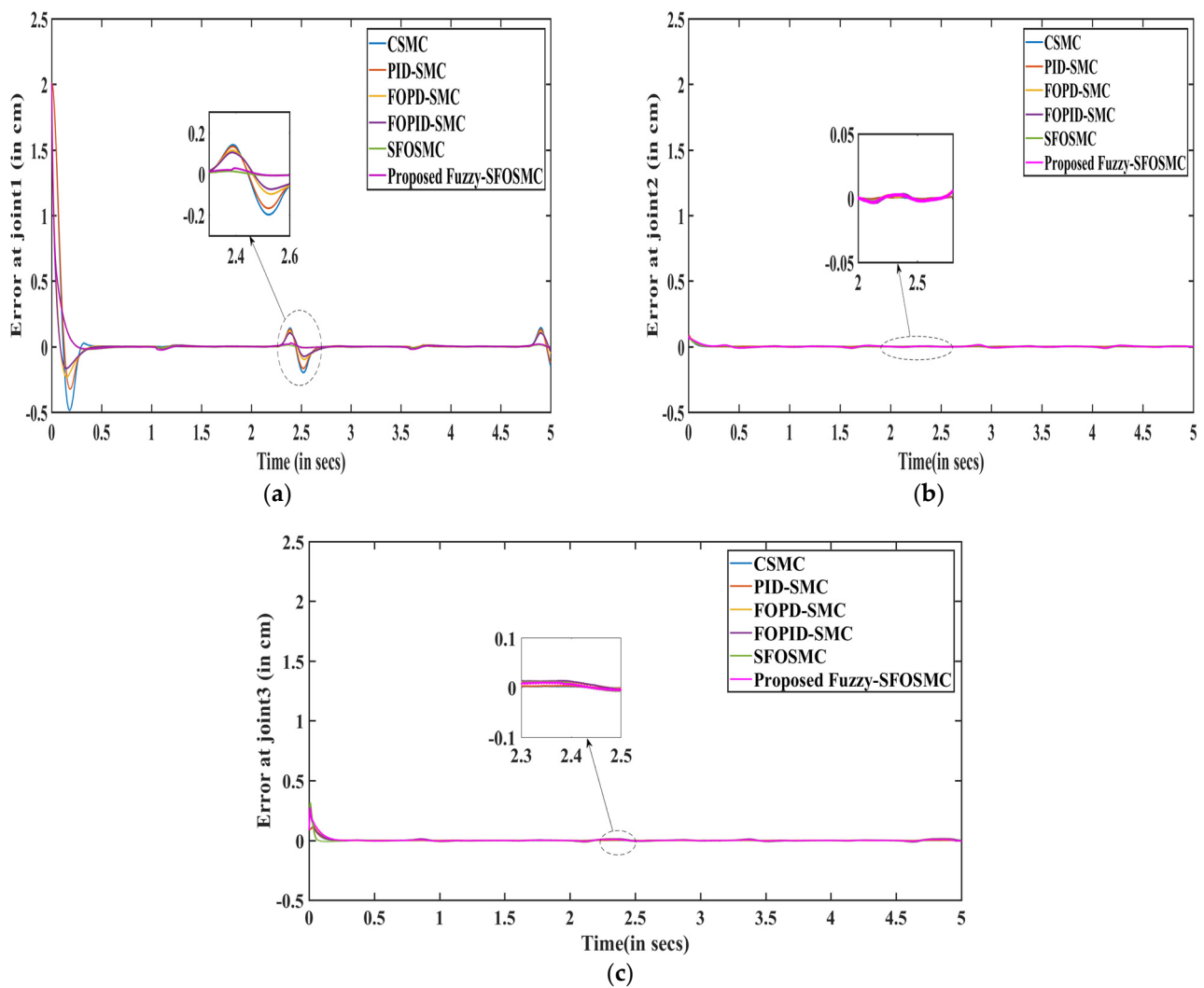
Figure 9. Trajectory tracking errors of the 3DOF surgical manipulator at Joint1 (**a**), Joint2 (**b**), and Joint3 (**c**).

Figure 10. *Cont*.

(**c**)
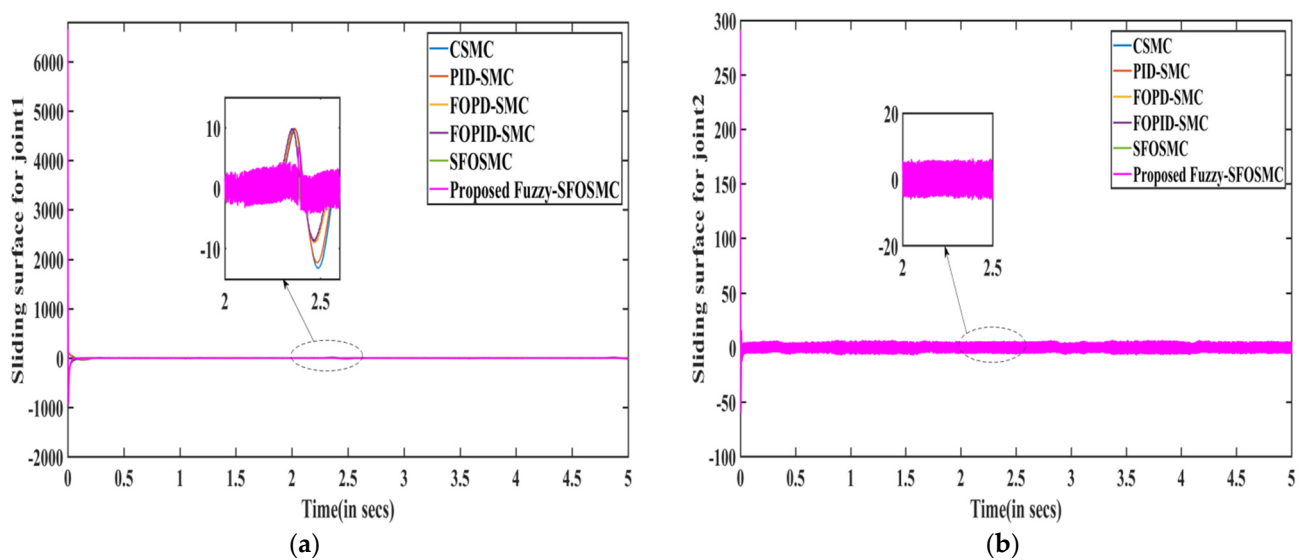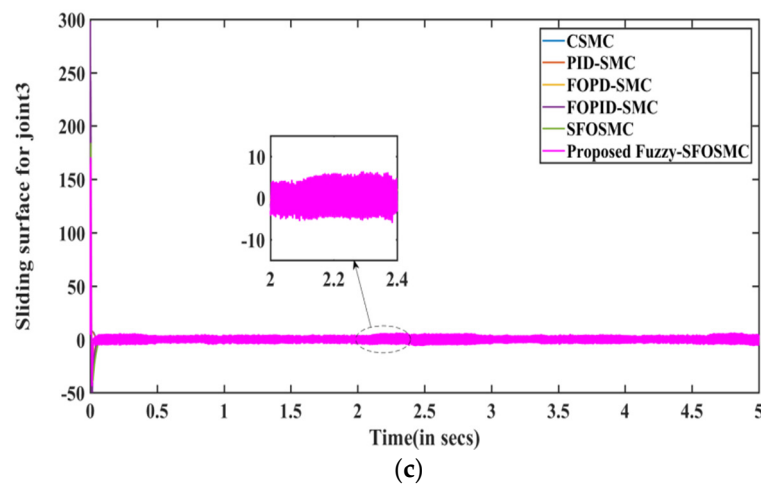
Figure 10. Sliding surfaces for Joint1 (**a**), Joint2 (**b**), and Joint3 (**c**) of the 3DOF surgical manipulator.

The simulation results of 3DOF surgical manipulator are shown in Figure 11, representing the controller output (τ) for Joint1, Joint2, and Joint3 of 3DOF surgical manipulator. It is observed that the proposed fuzzy-SFOSMC has minimal chattering compared to other controllers.

(**a**)

(**b**)

(**c**)
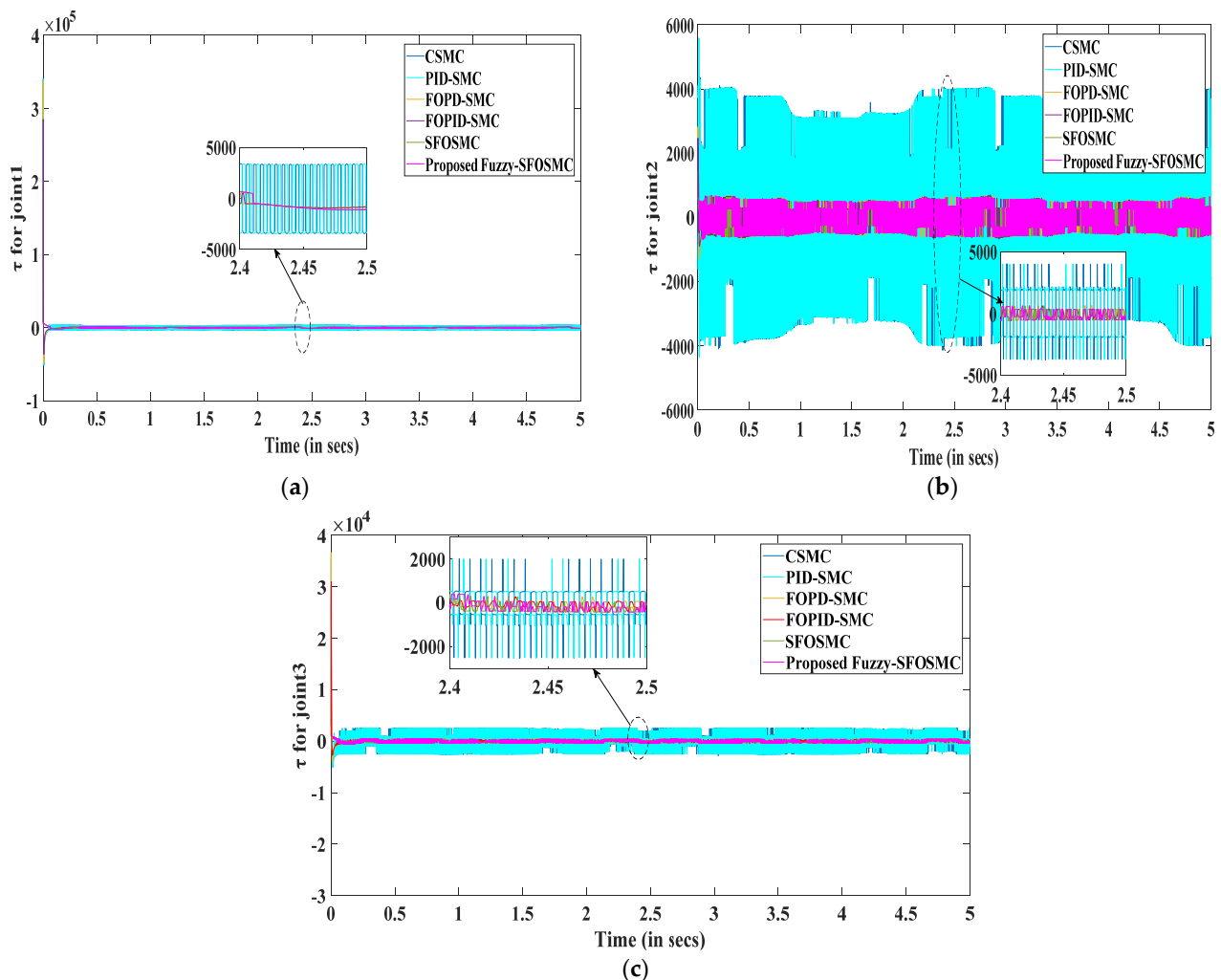
Figure 11. Controller output for Joint1 (**a**), Joint2 (**b**), and Joint3 (**c**) of the 3DOF surgical manipulator.

The time response parameters of various controllers for 3DOF surgical manipulator's joint1, i.e., the end-effector, are displayed in Table 2. It is observed that the proposed fuzzy-SFOSMC has greater precision, minimum overshoot, minimum integral square error (ISE), and better tracking compared to other controllers for nonlinear multi-incision trajectories, which are the primary requirements of a surgical robot. The SFOSMC has minimum undershoot. The achieved accuracy is less than 1mm, which is within the permissible limit. Similarly, similar parameters can be found for other joints. The gain parameters, found using PSO, of the discussed controllers are displayed in Table 3.

Table 2. Time response parameters of various controllers for 3DOF surgical manipulator's Joint1 for the 1st and 2nd cycle.

Controllers ＼ Specifications	First Cycle				Second Cycle				ISE (cm²)
	Rise Time (s)	Overshoot (%)	Undershoot (%)	Peak Time (s)	Rise Time (s)	Overshoot (%)	Undershoot (%)	Peak Time (sec)	
CSMC	0.078	24.2569	4.3633	0.180	0.162	7.1093	0.0204	2.536	0.2296
PID-SMC	0.085	16.1355	4.3633	0.185	0.164	5.5792	0.0096	2.537	0.2237
FOPD-SMC	0.063	11.4230	4.3633	0.153	0.170	2.8305	0.0922	2.558	0.0752
FOPID-SMC	0.060	8.1763	4.3633	0.151	0.172	2.0188	0.0904	2.574	0.0741
SFOSMC	0.120	1.0370	4.3633	0.344	0.173	0.1388	0.0901	2.683	0.0729
Proposed fuzzy-SFOSMC	0.1196	0.9293	4.3633	0.339	0.173	0.1141	0.1272	2.658	0.0710

Table 3. Gain parameters for different controllers.

CONTROLLERS	K_P	K_I	K_D	δ	μ
CSMC	50	0	2.1	-	-
PID-SMC	50	0.01	2.5	-	-
FOPD-SMC	50	0	2.1	-	1.2
FOPID-SMC	50	0.01	2.5	0.9	1.2
SFOSMC	50	0.01	2.5	0.9	1.2
Proposed fuzzy-SFOSMC	50	0.01	2.5	0.9	1.2

At times 0.6 s and 2.5 s, disturbances occur, causing the output characteristic to deviate from the desired characteristic, as shown in Figure 12. At 0.68 s and 2.6 s, the proposed fuzzy-SFOSMC controlled manipulator's response returns to the desired trajectory faster, indicating that the proposed controller has the minimum deviation from disturbances.
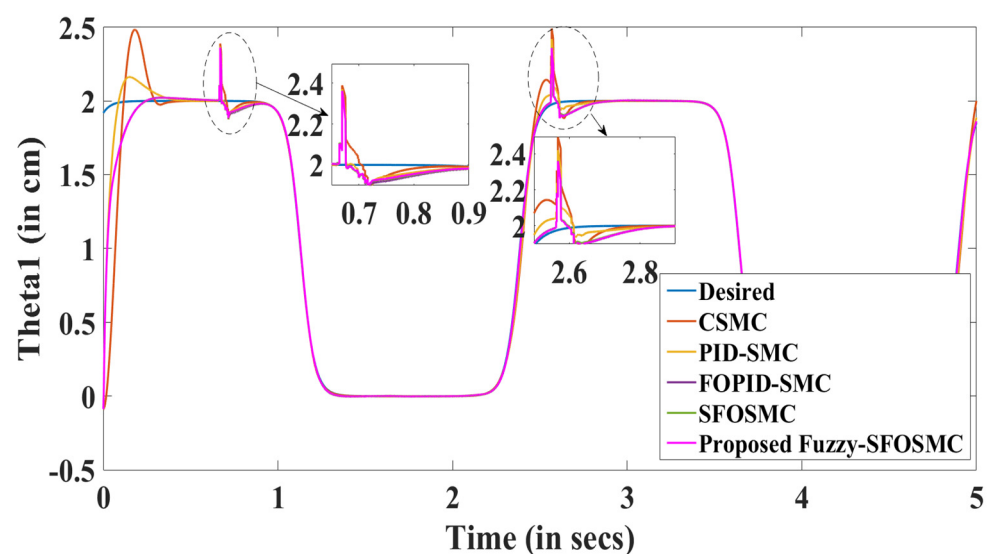

Figure 12. Trajectory tracking of the 3DOF surgical manipulator for Joint1 with disturbances.

5.2. Validation of Typical Situation during Surgery on OP5600

During surgery, motion control is very crucial. The simulation findings for this situation (explained in Section 5.1) were validated on Opal-RT OP5600. The experimental results for CSMC, PID-SMC, FOPD-SMC, FOPID-SMC, SFOSMC, and the proposed fuzzy-SFOSMC are illustrated in Figures 13–18, respectively. The following sub-figures show the desired trajectory (ϕ_d in cm), actual trajectory (ϕ in cm), tracking error (e in cm), and sliding surface (s) of all three joints of the 3DOF surgical manipulator. Figure 18 demonstrates that the proposed fuzzy-SFOSMC controlled 3DOF surgical manipulator has less tracking errors, less transients, less chattering, more precision, and better trajectory tracking than previous controllers, even for repeated identical motions and uncertainties, which are the primary requirements of a surgical robot.

(**a**)

(**b**)

(**c**)
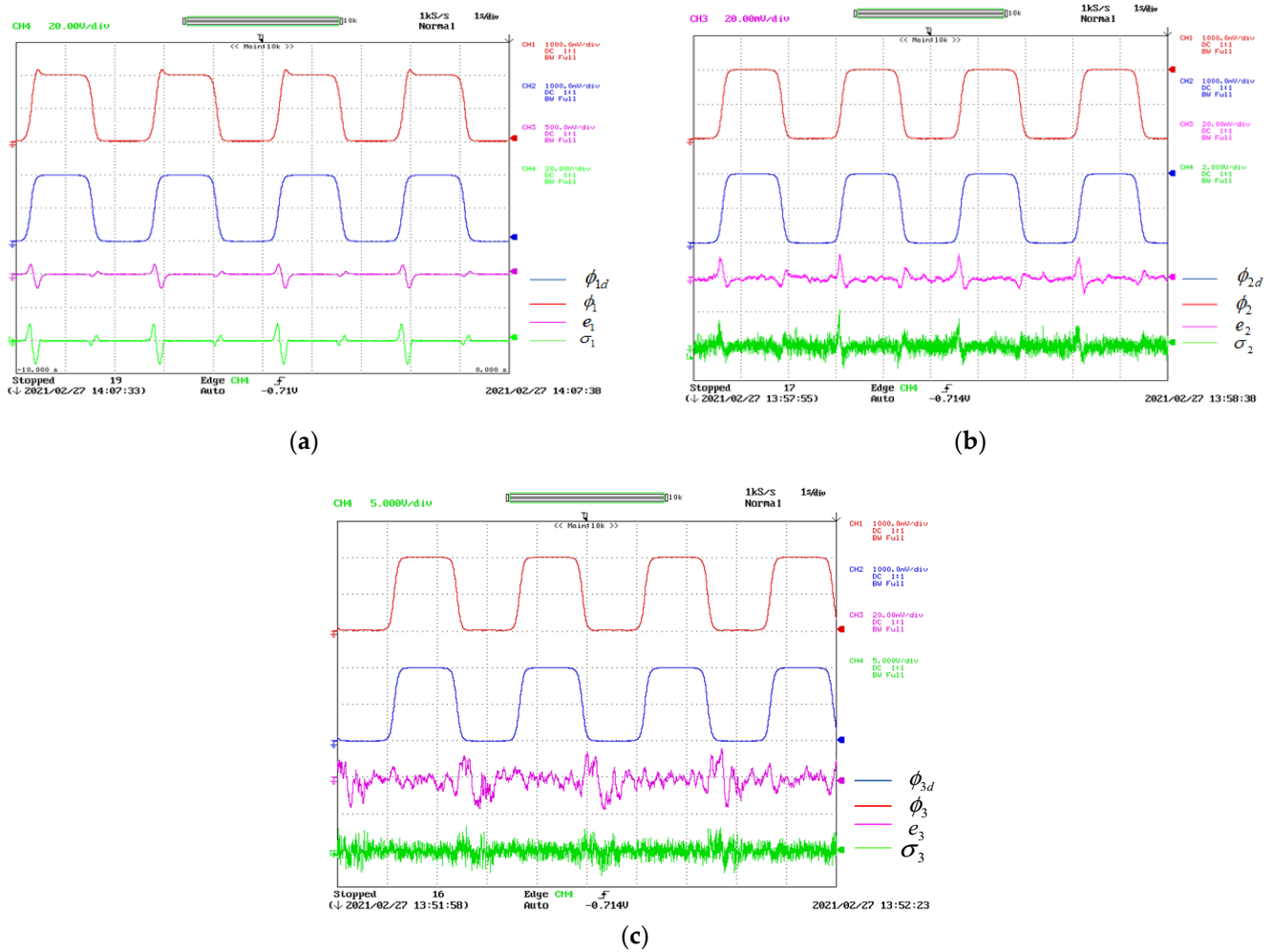
Figure 13. Trajectory tracking of the CSMC-controlled 3DOF surgical manipulator. (**a**) For Joint1 (**b**) For Joint2. (**c**) For Joint3.
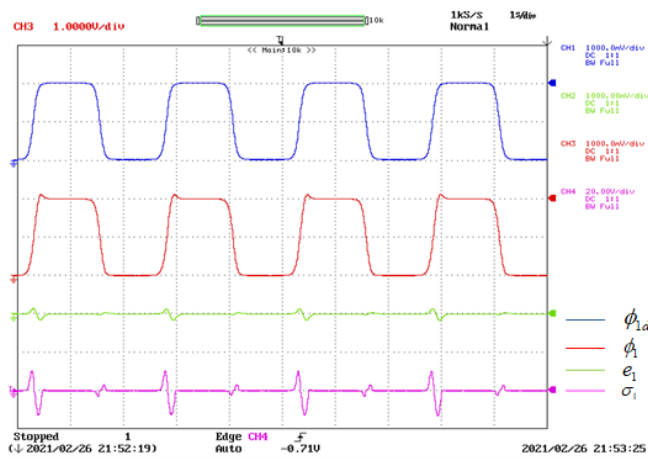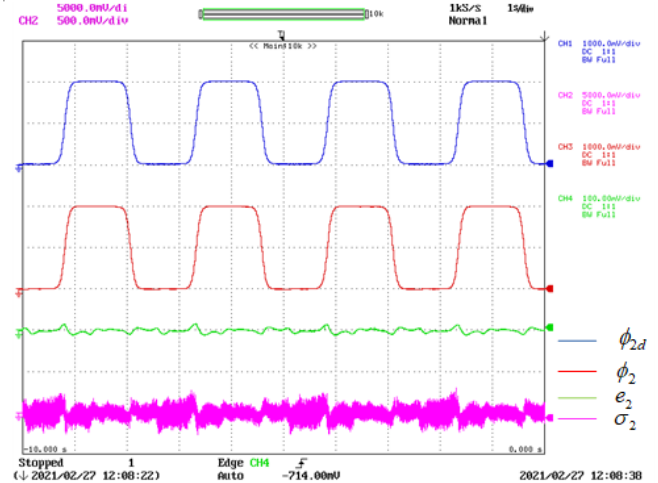
(**a**)
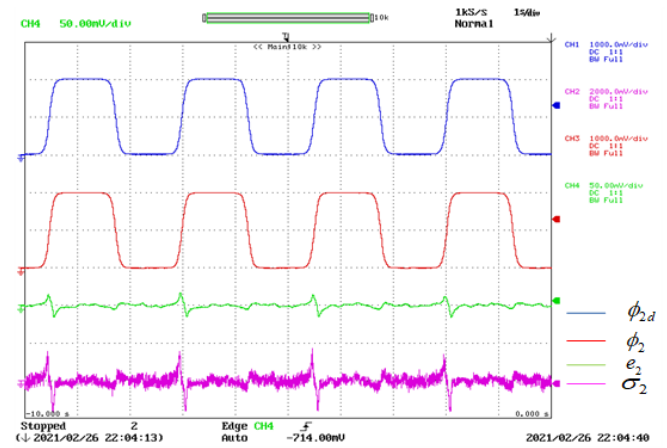
(**b**)
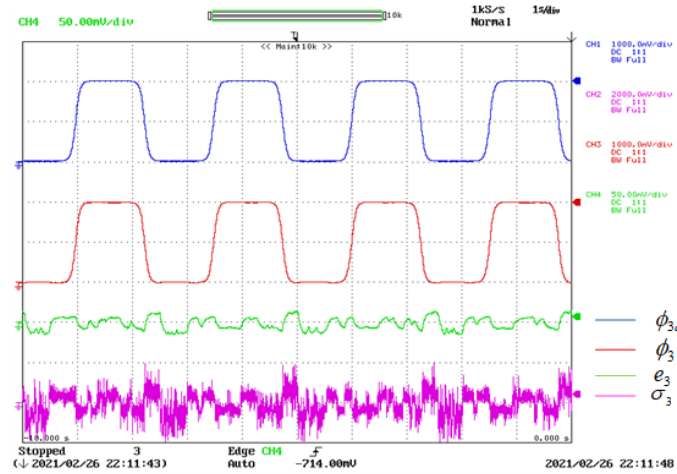
(**c**)

Figure 14. Trajectory tracking of the PID-SMC-controlled 3DOF surgical manipulator. (**a**) For Joint1 (**b**) For Joint2. (**c**) For Joint3.
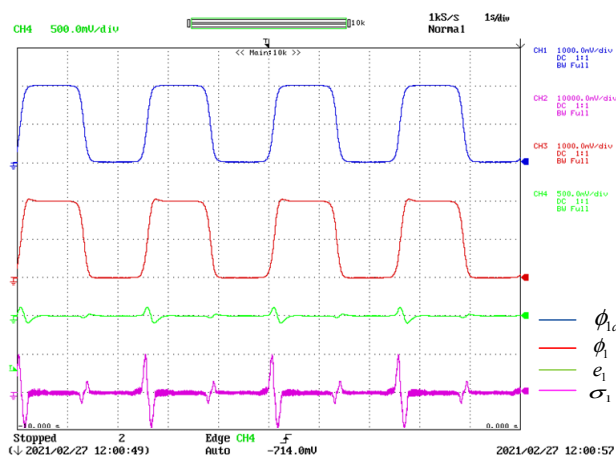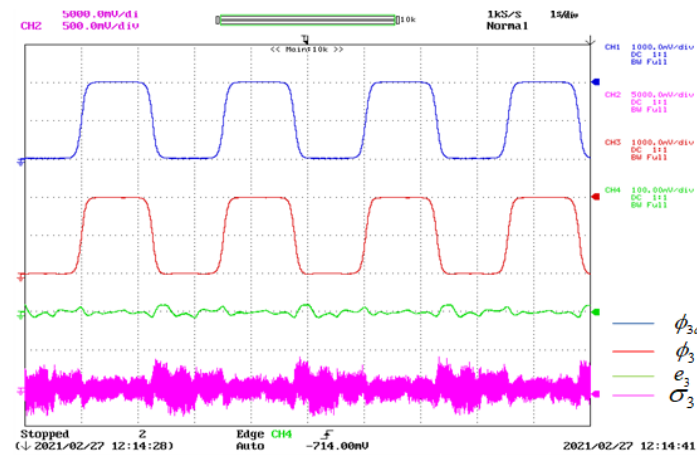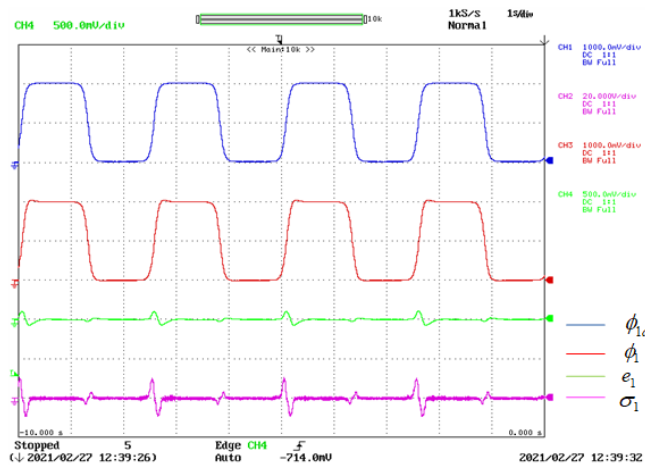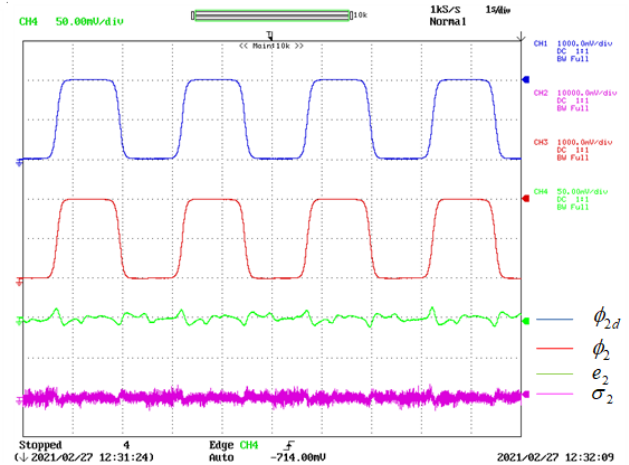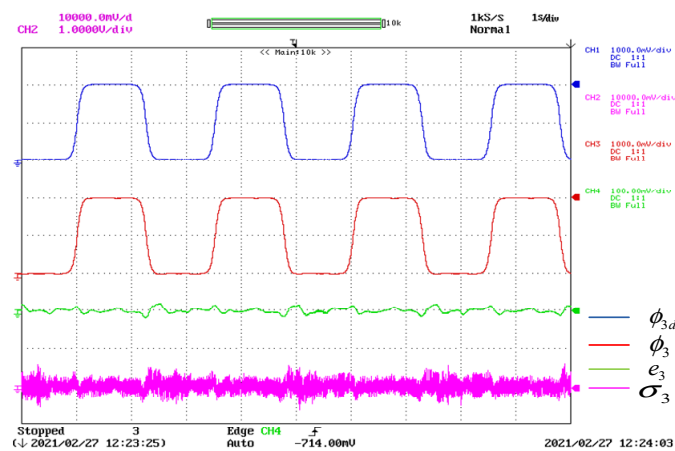

(**a**)

(**b**)

Figure 15. *Cont.*

(**c**)

Figure 15. Trajectory tracking of the FOPD-SMC-controlled 3DOF surgical manipulator. (**a**) For Joint1 (**b**) For Joint2. (**c**) For Joint3.

(**a**)

(**b**)

(**c**)

Figure 16. Trajectory tracking of the FOPID-SMC-controlled 3DOF surgical manipulator. (**a**) For Joint1 (**b**) For Joint2. (**c**) For Joint3.
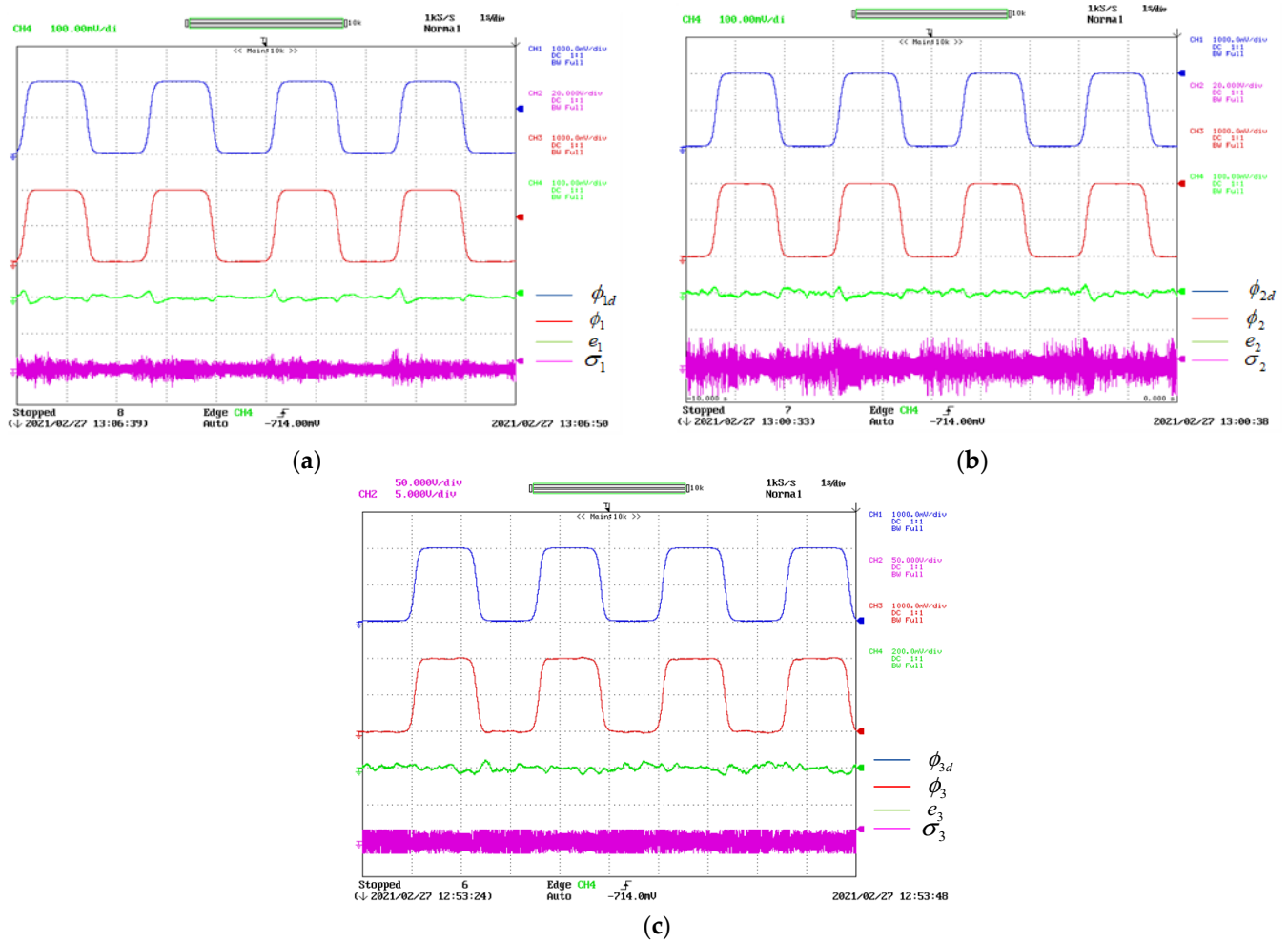
(**a**)

(**b**)

(**c**)

Figure 17. Trajectory tracking of the SFOSMC-controlled 3DOF surgical manipulator. (**a**) For Joint1 (**b**) For Joint2. (**c**) For Joint3.
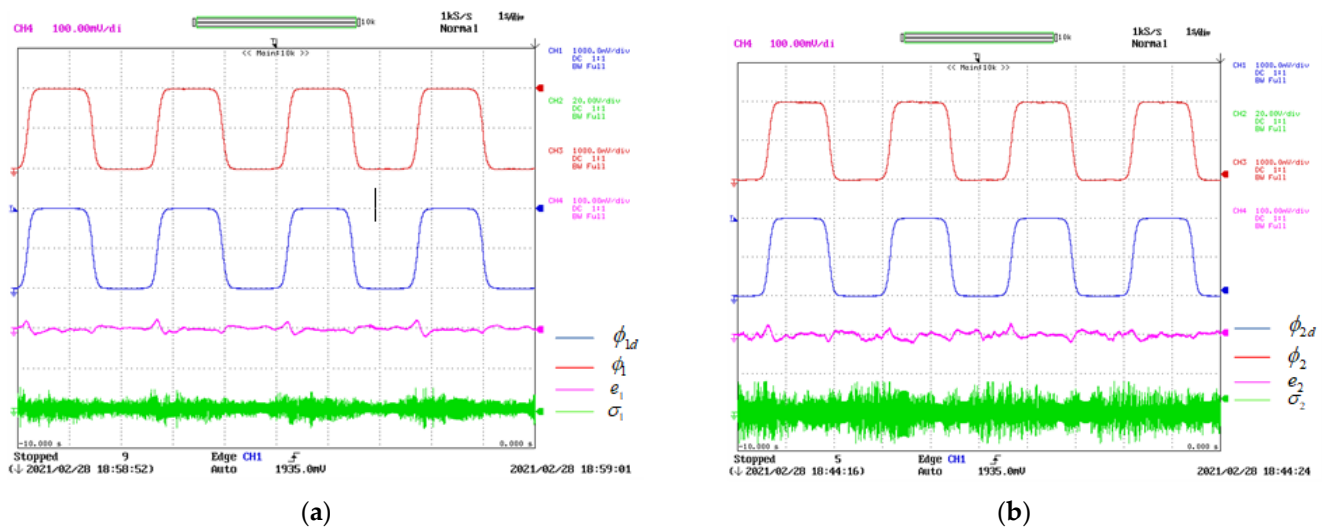

(**a**)

(**b**)

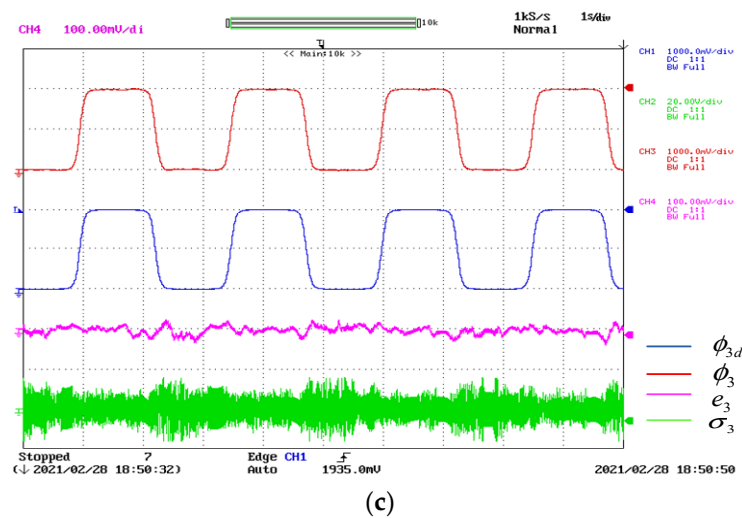**Figure 18.** *Cont.*

(c)

Figure 18. Trajectory tracking of the proposed fuzzy-SFOSMC-controlled 3DOF surgical manipulator. (**a**) For Joint1 (**b**) For Joint2. (**c**) For Joint3.

6. Conclusions

In this paper, various controllers for three-link surgical manipulators have been discussed. From the aforementioned findings, it can be inferred that the proposed fuzzy-SFOSMC controller for the slave robot follows the commands of the master robot efficiently. The CSMC controller has an overshoot of 24.25% and an undershoot of 4.3633%, which has been minimized to a significant degree, i.e., 0.11% and 0.12%, by using the fuzzy-SFOSMC controller. The achieved accuracy is less than 1mm, which is within the permissible limit. The proposed intelligent fuzzy-SFOSMC controller provides greater precision, stability, and robustness to time varying nonlinear multi-incision trajectories among all the controllers in the event of external disturbances and uncertainties, which are the primary requirements of surgical robots. Both simulation results and experimental results exemplify that the proposed controller has minimal tracking errors and better transient responses with less chattering than other conventional controllers.

References

1. Kawashima, K.; Kanno, T.; Tadano, K. Robots in laparoscopic surgery: Current and future status. *BMC Biomed. Eng.* **2019**, *1*, 12. [CrossRef] [PubMed]
2. Subido, E.D.; Pacis, D.M.; Bugtai, N.T. Recent technological advancements in laparoscopic surgical instruments. *AIP Conf. Proc.* **2018**, *1933*, 040007.
3. Corliss, W.R.; Johnsen, E.G. Teleoperator Controls. In *AEC-NASA Technology Survey*; NASA SP-5070; NASA Technology Utilization Division: Washington, DC, USA, 1968.
4. Qureshi, M.S.; Swarnkar, P.; Gupta, S. A supervisory on-line tuned fuzzy logic based sliding mode control for robotics: An application to Surgical Robots. *Robot. Auton. Syst.* **2018**, *109*, 68–85. [CrossRef]
5. Qureshi, M.S.; Kaki, G.N.; Swarnkar, P.; Gupta, S. Robust control techniques for master–slave surgical robot manipulator. *Harmon. Search Nat. Inspired Optim. Algorithms* **2018**, *741*, 599–609.

6.   Sachan, S.; Swarnkar, P. Design of smoothing FOPID sliding mode controlled robotic manipulator for Robotic-assisted Surgery. *Int. J. Recent Technol. Eng.* **2019**, *8*, 5002–5007. [CrossRef]

7.   Zhang, L.; Liu, L.; Wang, Z.; Xia, Y. Continuous finite-time control for uncertain robot manipulators with integral sliding mode. *IET Control Theory Appl.* **2018**, *12*, 1621–1627. [CrossRef]

8.   Slotine, J.J.E.; Li, W. *Applied Nonlinear Control*; Prentice Hall: Englewood Cliffs, NJ, USA, 1991.

9.   Piltan, F.; Sulaiman, N.; Rashidi, M. Design and implementation of sliding mode algorithm: Applied to robot manipulator-a review. *Int. J. Robot. Autom. (IJRA)* **2011**, *2*, 265–282.

10. Gopal, M. Nonlinear control structures. In *Digital Control and State Variable Methods*, 3rd ed.; Tata McGraw-hill: New Delhi, India, 2010; pp. 575–581.

11. Shah, P.; Agahse, S. Review of fractional PID controller. *Mechatronics* **2016**, *38*, 29–41. [CrossRef]

12. Varma, A.; Sachan, S.; Swarnkar, P.; Nema, S. Comparative analysis of conventional and meta-heuristic algorithm based control schemes for single link robotic manipulator. *Intell. Comput. Tech. Smart Energy Syst. (ICTSES) Proc. LNE* **2019**, *607*, 39–44. [CrossRef]

13. Tejado, I.; Djari, A.; Vinagre, B.M. Two strategies for fractional sliding mode control of integer order systems by system augmentation: Application to a servomotor. *IFAC Pap. OnLine* **2017**, *50*, 8103–8108. [CrossRef]

14. Zadeh, L.A. Fuzzy sets. *Inf. Control* **1965**, *8*, 338–353. [CrossRef]

15. Spong, M.W.; Vidyasagar, M. *Robot Dynamics and Control*; Wiley: New York, NY, USA, 1989.

16. Sarkhel, P.; Banerjee, N.; Hui, N.B. Fuzzy logic based tuning of PID controller to control fexible manipulators. *Springer Nat. Appl. Sci.* **2020**, *2*, 1124. [CrossRef]

17. Avazpour, M.R.; Piltan, F.; Ghiasi, H. Intelligent trajectory control of robotic-assisted surgery. *Int. J. Hybrid Inf. Technol.* **2015**, *8*, 73–90.

18. Wu, H.; Xu, Z. Fuzzy logic in decision support: Methods, applications and future trends. *Int. J. Comput. Commun. Control* **2020**, *16*, 1–28. [CrossRef]

19. Yang, Y.; Wu, J.; Zheng, W. Trajectory tracking for an autonomous airship using fuzzy adaptive sliding mode control. *J. Zhejiang Univ. SCIENCE C* **2012**, *13*, 534–543. [CrossRef]

20. Yang, Y.; Yan, Y.; Zhu, Z.; Zheng, W. Positioning control for an unmanned airship using sliding mode control based on fuzzy approximation. *Proc. Inst. Mech. Eng. Part G J. Aerosp. Eng.* **2014**, *228*, 2627–2640. [CrossRef]

21. Chen, G.; Jiang, Y.; Guo, K.; Wang, L. Speed Tracking Control for Unmanned Driving Robot Vehicle Based on Fuzzy Adaptive Sliding Mode Control. *IEEE Trans. Veh. Technol.* **2022**, *71*, 12617–12625. [CrossRef]

22. Lee, Y.J.; Bak, Y.; Lee, K.-B. Control Method for Phase-Shift Full-Bridge Center-Tapped Converters Using a Hybrid Fuzzy Sliding Mode Controller. *Electronics* **2019**, *8*, 705. [CrossRef]

23. Zhang, M.; Zhang, J. Fuzzy SMC Method for Active Suspension Systems with Non-ideal Inputs Based on a Bioinspired Reference Model. *IFAC-Pap.* **2022**, *55*, 404–409. [CrossRef]

24. Chen, W.; Xu, T.; Liu, J.; Wang, M.; Zhao, D. Picking Robot Visual Servo Control Based on Modified Fuzzy Neural Network Sliding Mode Algorithms. *Electronics* **2019**, *8*, 605. [CrossRef]

25. Qi, W.; Yang, X.; Park, J.H.; Cao, J.; Cheng, J. Fuzzy SMC for Quantized Nonlinear Stochastic Switching Systems With Semi-Markovian Process and Application. *IEEE Trans. Cybern.* **2022**, *52*, 9316–9325. [CrossRef] [PubMed]

26. Lin, H.; Yin, Y.; Shen, X.; Alcaide, A.M.; Liu, J.; Leon, J.I.; Vazquez, S.; Franquelo, L.G.; Wu, L. Fuzzy Logic System-Based Sliding-Mode Control for Three-Level NPC Converters. *IEEE Trans. Transp. Electrif.* **2022**, *8*, 3307–3319. [CrossRef]

27. Shami, T.M.; El-Saleh, A.A.; Alswaitti, M.; Al-Tashi, Q.; Summakieh, M.A.; Mirjalili, S. Particle Swarm Optimization: A Comprehensive Survey. *IEEE Access* **2022**, *10*, 10031–10061. [CrossRef]

28. Ouyang, P.; Pano, V. Comparative Study of DE, PSO and GA for Position Domain PID Controller Tuning. *Algorithms* **2015**, *8*, 697–711. [CrossRef]

29. Aguiar, A.L.S.; Sousa, F.B.C.; De Melo, Y.V.L. Optical Distribution Network Design using PSO. *IEEE Commun. Lett.* **2022**, *27*, 239–242. [CrossRef]

30. Chao, K.-H.; Hsieh, C.-C. Photovoltaic Module Array Global Maximum Power Tracking Combined with Artificial Bee Colony and Particle Swarm Optimization Algorithm. *Electronics* **2019**, *8*, 603. [CrossRef]